PROTEINS
STRUCTURE ■ FUNCTION ■ BIOINFORMATICS

Molecular modeling reveals binding interface of γ-tubulin with GCP4 and interactions with noscapinoids

Charu Suri,[1] Harish C. Joshi,[2] and Pradeep Kumar Naik[1]*

[1] Department of Biotechnology and Bioinformatics, Jaypee University of Information Technology, Waknaghat, Solan 173234, Himachal Pradesh, India

[2] Department of Cell Biology, Emory University School of Medicine, Atlanta, Georgia 30322

ABSTRACT

The initiation of microtubule assembly within cells is guided by a cone shaped multi-protein complex, γ-tubulin ring complex (γTuRC) containing γ-tubulin and atleast five other γ-tubulin-complex proteins (GCPs), i.e., GCP2, GCP3, GCP4, GCP5, and GCP6. The rim of γTuRC is a ring of γ-tubulin molecules that interacts, via one of its longitudinal interfaces, with GCP2, GCP3, or GCP4 and, via other interface, with α/β−tubulin dimers recruited for the microtubule lattice formation. These interactions however, are not well understood in the absence of crystal structure of functional reconstitution of γTuRC subunits. In this study, we elucidate the atomic interactions between γ-tubulin and GCP4 through computational techniques. We simulated two complexes of γ-tubulin-GCP4 complex (we called dimer1 and dimer2) for 25 ns to obtain a stable complex and calculated the ensemble average of binding free energies of −158.82 and −170.19 kcal/mol for dimer1 and −79.53 and −101.50 kcal/mol for dimer2 using MM-PBSA and MM-GBSA methods, respectively. These highly favourable binding free energy values points to very robust interactions between GCP4 and γ-tubulin. From the results of the free-energy decomposition and the computational alanine scanning calculation, we identified the amino acids crucial for the interaction of γ-tubulin with GCP4, called hotspots. Furthermore, in the endeavour to identify chemical leads that might interact at the interface of γ-tubulin-GCP4 complex; we found a class of compounds based on the plant alkaloid, noscapine that binds with high affinity in a cavity close to γ-tubulin-GCP4 interface compared with previously reported compounds. All noscapinoids displayed stable interaction throughout the simulation, however, most robust interaction was observed for bromo-noscapine followed by noscapine and amino-noscapine. This offers a novel chemical scaffold for γ-tubulin binding drugs near γ-tubulin-GCP4 interface.

Proteins 2015; 83:827–843.

Key words: γ-tubulin; gamma complex proteins; microtubule organization center; molecular modeling; molecular dynamics; MM-PBSA/MM-GBSA; alanine scanning mutagenesis; noscapinoids.

INTRODUCTION

Microtubules are hollow tube-like assemblies composed primarily of heterodimers of two globular protein subunits, α- and β- tubulin. These tubulin dimers associate in a head to tail fashion into linear protofilaments, 13–14 of which associated laterally constitute the tubular lattice of the microtubule. Within cells, microtubule assembly is initiated from multiprotein complex located at the microtubule organizing center.[1] The multiprotein complex contains a cone like γ-tubulin ring complex (γTuRC), involved in microtubule nucelation. γTuRC itself contains 6–7 copies of smaller tetrameric γ-tubulin small complexes (γTuSCs) composed of two copies of γ-tubulin and one of each of γ-tubulin-complex proteins 2 and 3 (GCP2 and GCP3).[2–10] However, the crystal structure of functional reconstitution of γTuRC subunits and their stepwise *in vitro* assembly from purified components is not yet possible. A recent 8 A° resolution cryo-electron microscopy density map of a tetramer

Additional Supporting Information may be found in the online version of this article.

The institution at which the work was performed: Department of Biotechnology and Bioinformatics, Jaypee University of Information Technology, Waknaghat, Distt. Solan 173234, Himachal Pradesh, India.

Grant sponsor: Jaypee University of Information Technology.

*Correspondence to: Pradeep Kumar Naik, Department of Biotechnology, Guru Ghasidas Vishwavidyalaya, A Central University, Koni, Bilaspur 495 009, Chhattisgarh, India. E-mail: pknaik1973@gmail.com

Received 30 July 2014; Revised 15 January 2015; Accepted 28 January 2015
Published online 7 February 2015 in Wiley Online Library (wileyonlinelibrary.com). DOI: 10.1002/prot.24773

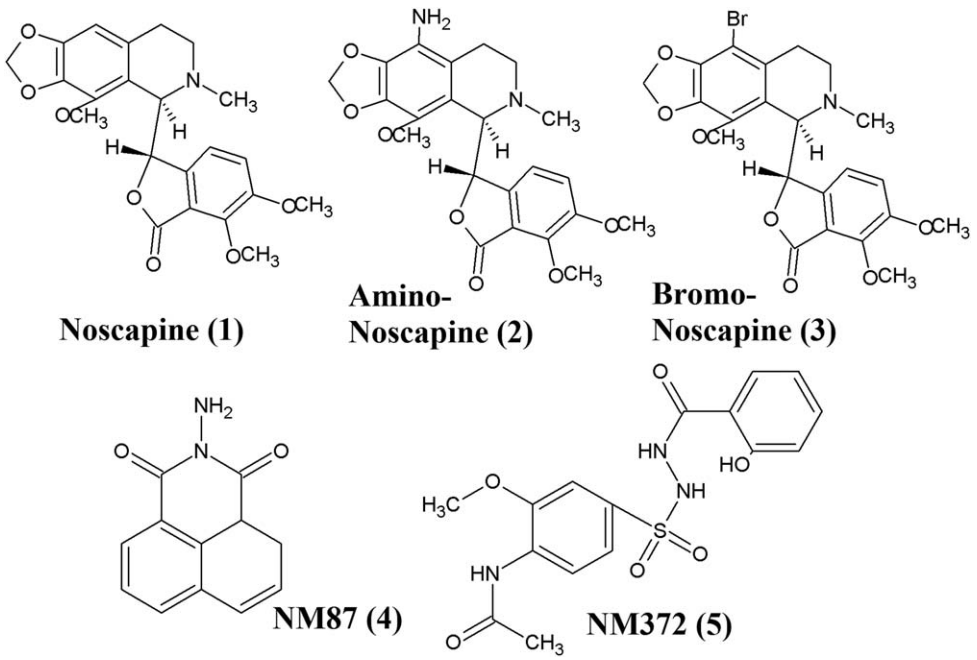

Figure 1

Molecular structure of the compounds: Noscapine (1), Amino-noscapine (2), Bromo-noscapine (3), and two reference compounds NM87 (4) and NM372 (5) used in the study. Both the reference compounds are previously reported to bind specifically onto the GCP4 and γ-tubulin interface.

subcomplex containing two heterodimers of γ-tubulin and GCP4[11] is a very welcome and timely beginning to investigate the assembly of γTuRC. Since γTuRC is crucial for microtubule assembly, it may serve as excellent targets for cancer chemotherapy as evident from the anti-cancer compounds that promote assembly (taxanes) or disassembly (vinca). These compounds disrupt microtubule spindle and ultimately cause apoptosis.

γ-tubulin is indispensible for the microtubule spindle function in mitosis and its absence causes cell death.[2,12] Recent studies have also indicated that γ-tubulin might also have a role in the regulation of microtubule dynamics at the plus ends.[13] Additionally, although tubulins (α/β) are abundant proteins constituting roughly 2.5% of the total protein in a cell, γ-tubulin makes up for <1% of the total tubulin content of the cell.[4] Higher expression of γ-tubulin has been associated with preinvasive lesions and carcinomas of the breast and prostate cancer, thyroid carcinomas and glioblastoma multiforme.[14–19] Therefore, γ-tubulin has a clearly high potential of proving to be an excellent drug target for cancer therapy. Therefore, there is intense interest in developing promising leads that interfere with its function. There are multiple approaches to this end. For example, using a fragment based approach combined with biophysical screening of several small molecules; Cala *et al.* (2013) identified potential γ-tubulin interacting agents preferably at the γ-tubulin-GCP4 binding interface.[20] This approach has lead to some promising leads, like NM87 and NM372, which we have also used as references in our study (Fig. 1).

Advances in the crystal structures of alpha-, beta-, and gamma-tubulins yielded a realization that the overall structure of γ-tubulin was more similar to β-tubulin subunit than it is to the α-tubulin subunit.[21–24] Because β-tubulin has a very well characterized drug binding cavities, one straight approach is to explore how well these cavities are conserved in γ-tubulin structure and whether they can be used to identify potential lead compounds that can bind these cavities. To this end, Friesen *et al.* (2012) performed a rigorous search for colchicine binding site within the structure of γ-tubulin.[25] The colchicine site also accommodates many structurally related compounds such as podophyllotoxin and combrestatin. Not only did they find that the colchicine site is conserved between β-tubulin and γ-tubulin, but they showed that bacterially expressed γ-tubulin binds colchicine with a dissociation constant of 13.9 μ*M* compared with a dissociation constant of 1.1 μ*M* with β-tubulin suggesting that this is a good lead.[25] Colchicine and podophyllotoxin however, have been of limited use for cancer therapy because they are too toxic to animals at cancer therapeutic doses. Based on the structures of colchicine, podophyllotoxin, combrestatin like compounds, Ye *et al.* (1998) identified a natural plant alkaloid noscapine.[26] Several higher affinity analogues (noscapinoids) were then developed and shown to compete with the

colchicines.[27] These compounds modulate microtubule dynamics upon binding and induce apoptosis both during mitosis and during interphase of the cell cycle.[28,29] More importantly, perhaps due to milder effect on the normal cells, they do not display major side effects due to the disruption of hematopoiesis, hair follicles, gastrointestinal lining and the axonal transport and integrity. For example, Phase I/II studies showed low toxicity even at high dose of 300 mg/kg body weight.[30] It will therefore be of major interest to investigate if this class of compounds can also interact against γ-tubulin or against any of its associated γ-tubulin complex proteins.

In this study, we first strive to extensively use molecular modelling and molecular dynamics (MD) simulation techniques to investigate the precise mode of interaction between GCP4 and γ-tubulin. We than investigated whether noscapinoids bind specifically at the interface of γ-tubulin and GCP4 proteins using molecular docking, MD simulation and followed by molecule mechanics Poisson Boltzmann surface area (MM-PBSA) and Generalized Borne surface area (MM-GBSA). Furthermore, we have used two previously reported compounds, NM372 and NM87, which were demonstrated to bind at the interface of γ-tubulin and GCP4 proteins[20] to compare and contrast the binding affinity of noscapinoids.

MATERIALS AND METHOD

Molecular insight between GCP4 and γ-tubulin interaction

Model building of the γ–tubulin-GCP4 complex

In the absence of crystal structure of γ-tubulin-GCP4 complex, we have reconstituted their dimer complex and used in our study. A structure file consisting of atomic coordinates of the GCP4 and γ-tubulin tetramer was obtained from Georges Czaplicki, from the Université de Toulouse, UPS, Toulouse, France. This molecular structure has not been determined using X-ray crystallography technique and was generated as reported earlier.[20] Briefly the crystal structures of GCP4 (PDB code 3RIP) and human γ-tubulin (PDB code 3CB2) were fitted into the 8 Å cryo-electron microscopy (EM) reconstruction of the *Saccharomyces cerevisiae* γ-tubulin small complex (γ-TuSC)[20] to obtain the tetramer complex structure of GCP4 and γ-tubulin. GCP4 was fitted remarkably well into the γ-TuSC cryo-EM structure. Some manual adjustments were carried out in the bend angle between the third and fourth helical bundles with relative arrangements of N- and C-terminal domains. The missing loops in the original GCP4 crystal structure were gap filled using the SuperLooper Web Server. Finally, a simulation of MD for 10ns was performed to allow the structure to relax and to adopt a preferential conformation in the complex. This tetramer complex structure of GCP4 and γ-tubulin we obtained from Georges Czaplicki was split into two dimer complex of GCP4 and γ-tubulin (we called dimer1 and dimer2). Each of this complex was then prepared using protein preparation wizard (PPrep) workflow in Schrodinger package. During protein preparation all the water molecules were removed from the complex, missing hydrogen atoms were added to the structure using Maestro interface (version 9.2, Schrödinger) and hydrogen bonds were optimized. Missing side chains were filled using Prime (version 3.0, Schrodinger, LLC). Finally, the structure was energy minimized using Macromodel (Schrodinger). The minimization was done with Polak-Ribiere Conjugate Gradient algorithm. The minimization was stopped either after 5,000 steps or after the energy gradient converged below 0.001 kcal/mol.

MD simulation of GCP4 and γ-tubulin complex

Both the dimer complexes of GCP4 and γ-tubulin were subjected to all atom MD simulations to verify the stability of the complex during a long MD run of 25 ns and also to calculate the ensemble average of binding free energy between GCP4 and γ-tubulin from the MD trajectories. The MD simulations were performed with the Amber 11.0 software and Ambertools 1.5.[31,32] Tleap program implemented in Amber 11 was used to assign parameters from FF99SB force field to the molecular system. The systems were then neutralized and solvated using TIP3P model to finally generate the toplogy and coordinate files.[33–35] The complex of GCP4 and γ-tubulin was subjected to three consecutive rounds of 1000 step minimization employing 500 steps of steepest descent followed by 500 steps of conjugate gradient methods. For the first and second rounds only water molecules were relaxed while the protein was held fixed using force constants of 10 and 2 kcal mol^{-1} $Å^{-2}$, respectively. In the third round, the entire system was allowed to relax without any restraint. The fully relaxed structure was then heated to 300 K in 100 ps. The system was subjected to density equilibration over 100 ps followed by 500 ps of constant pressure equilibration at 300 K and 1 atm pressure with a force constant of 2 kcal mol^{-1} $Å^{-2}$. A 25 ns MD simulation was carried out on the equilibrated system using Particle Mesh Ewald MD method using the time step of 2 fs.[36,37] Through out the simulation the Langevin thermostat was used to regulate the temperature and the bond lengths involving hydrogen bonds were constrained using SHAKE algorithm.[38] MD was carried out in an NPT ensemble using a Berendsen barostat[39] with a target pressure of 1 atm. The structures were recoreded every 1 ps resulting in a trajectory with 25,000 frames. All trajectories were analysed using PTRAJ program implemented in Ambertools.

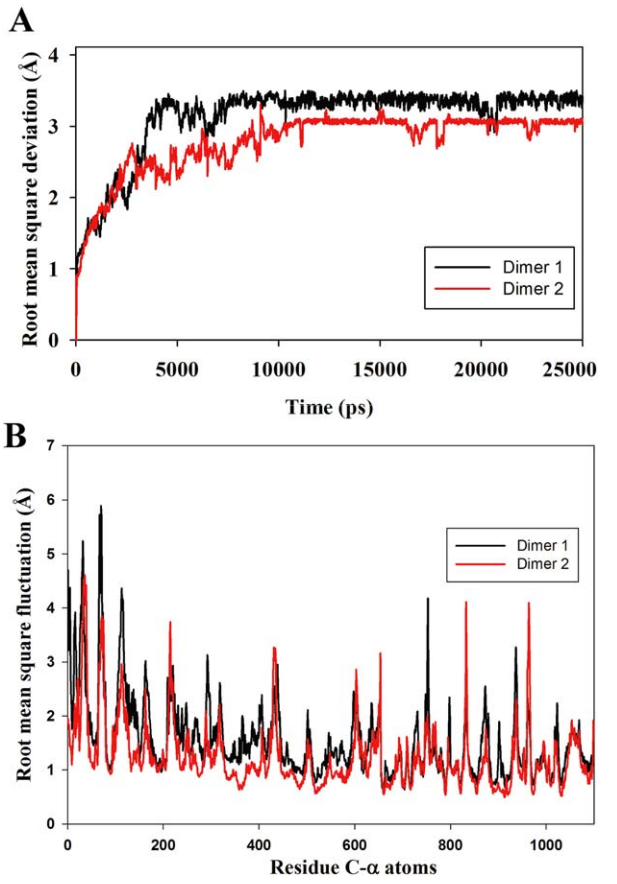

Figure 2

Root mean square daviation (RMSD) and root mean square fluctuation (RMSF) of Cα atoms of GCP4 and γ-tubulin complex. **A**: The RMSD of Cα atoms in the GCP4 and γ-tubulin complex in dimer1 and dimer2 over 25 ns. The relative fluctuation in the RMSD of the Cα atoms is very small after 5000 ps, revealed that each system reaches equilibrium at 5000 ps. **B**: The RMSF of Cα atoms of residues in the GCP4 and γ-tubulin complex in dimer1 and dimer2 over a period of 25 ns MD simulation. The residues with higher RMSF tend to show more flexibility. [Color figure can be viewed in the online issue, which is available at wileyonlinelibrary.com.]

Calculation of binding free energy between GCP4 and γ-tubulin

The intermolecular binding free energy between GCP4 and γ-tubulin in solvation was carried out using the conventional MM-PBSA and MM-GBSA approaches using Amber 11.[40,41] A total of 500 snapshots were extracted, every 10 ps from the last 5 ns of the MD trajectory and used for the calculation of ensemble average of binding free energy. The binding free energy for each snapshot was calculated as follows.

$$\Delta G_{\text{bind}} = \Delta G_{\text{complex}} - \left[\Delta G_{\text{Rec}} + \Delta G_{\text{lig}}\right] \quad (1)$$

The free energy, *G*, for each molecular species was calculated by the following scheme using the MM-PBSA and MM-GBSA methods described in Amber 11:

For each molecular species, Gibbs's free energy (G) was calculated as follows.

$$G = E_{\text{gas}} + G_{\text{sol}} - TS \quad (2)$$

where E_{gas} is the gas phase energy calculated as the sum of internal energy, energy generated as a result of the electrostatic interaction and the van der Waals interaction. The E_{gas} was calculated using parameters from FF99SB force field.[33,34]

$$E_{\text{gas}} = E_{\text{int}} + E_{\text{ele}} + E_{\text{vdw}} \quad (3)$$

G_{sol} is the solvation free energy, which was calculated as the sum of polar and nonpolar contributions as

$$G_{\text{sol}} = G_{\text{PB(GB)}} + G_{sol\text{-}np} \quad (4)$$

where $G_{\text{PB(GB)}}$ is the polar solvation contribution calculated by solving the PB and GB equations.

Polar interaction contribution was calculated as the summation of electrostatic contribution and polar solvation contribution.

$$G_{\text{ele,PB(GB)}} = E_{\text{ele}} + G_{\text{PB(GB)}} \quad (5)$$

The nonpolar solvation contribution ($G_{\text{sol-np}}$) is approximated as linearly dependent on the solvent accessible surface area (SAS), which was determined using a water probe radius of 1.4 Å, surface tension constant γ was set to 0.0072 kcal mol^{-1} Å^{-2}.[42]

$$G_{\text{sol-np}} = \gamma SAS \quad (6)$$

Dielectric constant for solute and solvent were set to 1 and 80, respectively. T and S are the temperature and the total solute entropy.

Per residue energy contribution

To identify those residues, which play a more substantial role in the binding of GCP4 with γ-tubulin, energy contribution of each amino acid in the complex was determined. For this energy decompostion method, implemented in Amber 11, was employed on the 500 frames extracted every 10 ps from the last 5 ns of MD trajectory using the MM-GBSA method. The residues contributing <-3 kcal/mol were considered very significant for the binding of GCP4 with γ-tubulin and these residues were designated as hotspot amino acids.

Alanine scanning mutagenesis

To further verify the energy contribution of these hotspot residues in the interaction of GCP4 and γ-tubulin, computational alanine scanning was performed. In this method, an amino acid of interest is replaced with

Table I
Calculated Binding Free Energy Between GCP4 and γ-Tubulin

Contribution	Dimer1 (kcal/mol)	Dimer2 (kcal/mol)
ΔE_{INT}	0.00	0.00
ΔE_{VDW}	−259.46	−195.71
ΔE_{ELE}	−100.47	96.576
ΔE_{GAS}	−359.93	−99.134
ΔG_{PB}	224.34	−11.954
$\Delta G_{SOL\text{-}NP}$	−168.24	−115.50
$\Delta G_{SOLV,PB}$	201.11	19.601
$\Delta G_{ELE,PB}$	123.87	84.621
$\Delta G_{bind,PBSA}$	−158.82	−79.533
ΔG_{GB}	221.44	19.075
$\Delta G_{SOLV,GB}$	189.74	−2.3638
$\Delta G_{ELE\ GB}$	120.97	115.65
$\Delta G_{bind,GBSA}$	−170.19	−101.50

Binding free energy calculated using MM-GBSA and MM-PBSA to ascertain the strength of interaction between GCP4 and γ-tubulin for both dimer1 and dimer2. The major energy components like van der Waals, electrostatic, polar salvation, and nonpolar solvation, contributing to the binding free energy were also estimated.

alanine and absolute binding free energy is recalculated. In our study, the hotspot residues were mutated to alanine and binding free energies were calculated for the resulting mutated system using the MM-GBSA approach on the 500 snapshots extracted every 10 ps from the last 5 ns of MD simulation. Finally, the difference in the binding free energies of the mutant and wild type, $\Delta\Delta G_{bind}$ was computed as follows:

$$\Delta\Delta G_{bind} = \Delta G_{bind}[\text{Mutant}]\_\Delta G_{bind}[\text{Wild type}] \quad (7)$$

Positive values of $\Delta\Delta G_{bind}$ indicate the favourable contribution while negative values indicate unfavourable contributions.

Molecular interaction of noscapinoids onto GCP4 and γ-tubulin interfaces

Ligand preparation

The molecular structure of the lead molecule, noscapine and two of its derivatives such as amino-noscapine and bromo-noscapine **1-3** (Fig. 1) were built using molecular builder of Maestro (version 8.5, Schrodinger LLC). We also selected and built two compounds, NM87 and NM372 **4,5** (Fig. 1) as reference compounds, which have previously reported to bind specifically to the GCP4 and γ-tubulin interface.[20] All these five structures **1-5** were energy minimized in vacuo using Impact (version 5.6, Schrodinger, LLC). Appropriate bond orders were assigned to each structure using Ligprep (version 2.4, Schrodinger LLC) and initial optimization was performed on each structure by employing OPLS 2005 force field using default setting. Furthermore, geometrical optimization of these ligands was performed in Jaguar (version 7.7, Schrodinger, LLC) using hybrid density functional theory with Becke's three-parameter exchange potential and the Lee–Yang–Parr correlation functional (B3LYP)[43,44] using basis set 3-21G* level.[45–47]

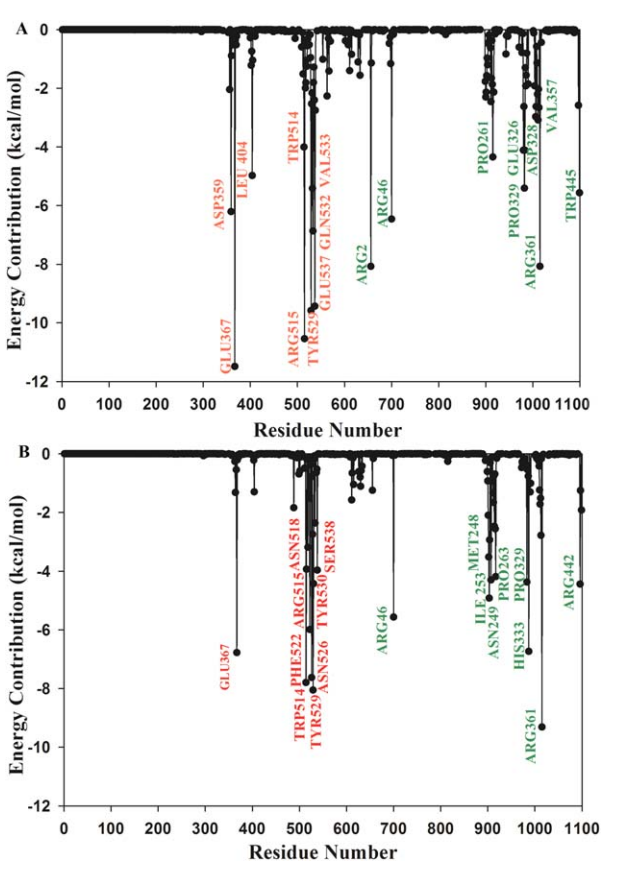

Figure 3
Per residue free energy contribution of residues in the binding process of GCP4 and γ-tubulin. Free energy contribution of each residue on the surface between GCP4 and γ-tubulin involve in the interaction in (**A**) dimer1 and (**B**) dimer2 calculated based on MM-GBSA. Only the residues contributing free energy of <-3 kcal/mol (designated as hotspot amino acids) are labeled in the figure. The hotspot residues belonging to GCP4 are labeled red while those of γ-tubulin are labeled green. [Color figure can be viewed in the online issue, which is available at wileyonlinelibrary.com.]

Molecular docking

The average structure of GCP4 and γ-tubulin complex was generated out of 500 snapshots extracted every 10 ps from the last 5 ns of the MD trajectory and used in molecular docking of ligands. All possible binding sites of GCP4 and γ-tubulin complex were predicted and analyzed using SiteMap software (version 2.4, Schrodinger). For comparative analysis, only those binding sites which consist of at least 5 site points were considered. Docking studies were performed using Glide (version 4.5, Schrodinger, LLC). A grid box size of 10 Å each for the bounding and enclosing boxes were generated, placing the centroid of the predicted binding site of the GCP4 and γ-tubulin to be at the center of

Table II
Energy Decomposition

Chain	Residue	$\Delta E_{i,vdw}$ (Kcal/mol)	$\Delta E_{i,ele}$ (Kcal/mol)	$\Delta G_{i,sol\ GB}$ (Kcal/mol)	$\Delta G_{i,sol\text{-}np}$ (Kcal/mol)	$\Delta G_{i,bind,GB}$ (Kcal/mol)
(a) Dimer1						
GCP4 (Chain A)	ASP359	−0.73	18.73	−24.09	−0.12	−6.21
	GLU367	−1.37	1.04	−10.17	−0.87	−11.37
	LEU404	−3.67	0.13	−0.63	−0.81	−4.98
	TRP514	−4.04	−1.12	1.87	−0.71	−4.31
	ARG515	−4.08	−92.44	86.94	−0.96	−10.54
	TYR529	−5.71	−14.66	11.07	−0.37	−9.67
	GLN532	−7.65	−9.68	13.13	−1.21	−5.41
	VAL533	−6.01	−4.57	5.18	−1.47	−6.87
	GLU537	−3.01	−1.61	−4.16	−0.67	−9.45
γ-tubulin (Chain B)	ARG2	−1.05	−85.95	79.01	−0.08	−8.07
	ARG46	−2.36	−97.03	93.56	−0.81	−6.64
	PRO261	−3.82	−6.01	6.45	−0.95	−4.33
	GLU326	−2.75	30.44	−30.90	−0.88	−4.09
	ASP328	−3.47	41.11	−42.29	−0.87	−4.22
	PRO329	−4.74	−3.98	5.00	−0.50	−5.52
	VAL357	−1.65	−3.76	2.73	−0.42	−3.16
	ARG361	−1.40	−68.13	61.06	−0.70	−9.17
	TRP445	−5.51	−38.32	40.29	−1.23	−5.27
(b) Dimer2						
GCP4 (Chain A)	GLU367	−2.06	29.60	−33.69	−0.58	−6.73
	TRP514	−7.71	−4.56	6.44	−1.89	−7.72
	ARG515	−3.57	−80.93	82.10	−1.45	−3.84
	ASN518	−3.88	−7.01	8.68	−0.96	−3.17
	PHE522	−6.70	−1.61	4.40	−1.89	−5.79
	ASN526	−5.11	−10.57	8.41	−0.47	−7.74
	TYR529	−6.87	−5.79	7.29	−2.56	−7.92
	TYR530	−5.35	−2.80	4.58	−0.99	−4.57
	SER538	−2.05	−4.50	3.02	−0.44	−3.97
γ-tubulin (Chain B)	ARG46	−3.50	−62.16	60.89	−0.78	−5.55
	MET248	−5.14	−0.71	3.27	−0.95	−3.52
	ASN249	−6.66	−9.03	12.82	−1.89	−4.76
	ILE 253	−4.50	−0.94	2.15	−0.98	−4.28
	PRO263	−4.49	1.08	−0.30	−0.37	−4.08
	PRO329	−3.95	−2.72	3.11	−0.76	−4.32
	HIS333	−4.52	−10.64	9.71	−1.25	−6.69
	ARG361	−2.66	−75.22	69.56	−0.85	−9.16
	TYR442	−1.63	−8.70	6.21	−0.24	−4.36

Decomposition of calculated $\Delta G_{bind,GB}$ (kcal/mol) on per residue basis into van der Waals, electrostatic, polar solvation and nonpolar solvation energy components for the hotspot amino acids. Those amino acids which contributed < -3 kcal/mol to the binding free energy of GCP4 and γ-tubulin complex were considered as hotspot amino acids.

the grid box. The receptor-grid file was generated using grid receptor generation program with van der Waals scaling of 0.4 Å.The ligands were first docked using the "standard precision" method and further refined using "extra precision" Glide algorithm.[48–50] Van der Waals scaling of the ligand was set at 0.4 Å for all docking experiments. Out of the 50,000 poses that were sampled, 4,000 were subjected to energy minimization using conjugate gradients method over 1,000 steps. A total of thirty structures with lowest energy conformations were then screened for favourable Glide docking score. Single best conformation for each ligand–protein complex was selected for further molecular modeling calculations.

Structure preparation of docked complexes

The complexes obtained after molecular docking required some structure preparation to make them suitable for MD simulations in Amber 11. The missing parameters for all five ligands were estimated with the antechamber programs[51] implemented in Amber 11. AM1-BCC charge model was used to calculate the atomic point charges.[52] Missing hydrogens were added and FF99SB forcefield was employed to assigned parameters to the complex of GCP4 and γ-tubulin, while GAFF forcefield was used to assigned the parameters to each ligand using tleap module available in Amber 11. Each system was neutralized using sodium ions and solvated using TIP3 water model in a truncated octahedron with distance of at least 15 Å between the wall of the box and the closest atom of the complex.[35]

MD simulation of docked complexes

The parameter for the compounds **1-5** were estimated using antechamber program in Amber 11 simulation

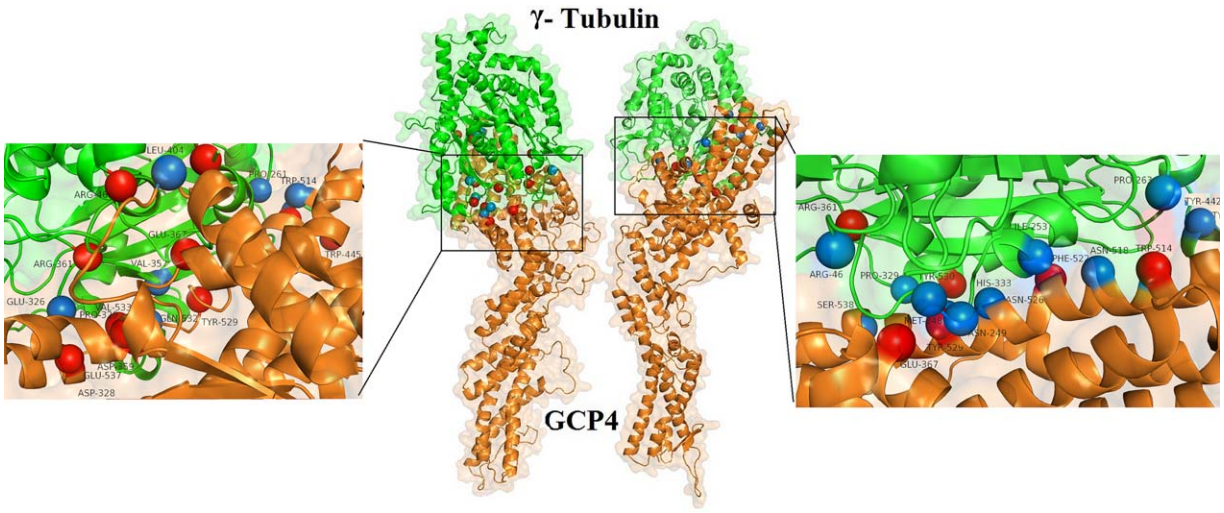

Figure 4

Spatial distribution of hotspot residues at the binding interface. Hotspot residues involve in the binding process of GCP4 and γ-tubulin at the interface in the dimer1 (**A**) and dimer2 (**B**) are represented in the three dimensional space model of the complex. The hotspot residues contributing free energy of <-5 kcal/mol are marked red, while the residues contributing free energy in between -3 and -5 kcal/mol are marked blue. In total 18 residues each on the surface of GCP4 and γ-tubulin involve in the binding process in both dimer1 and dimer2. However, the residues are albeit different between both the dimers. This is the reason that the predictive binding free energies between both the dimers are different. The binding free energy between GCP4 and γ-tubulin calculated in dimer1 is much higher (-170.19 and -158.82 kcal/mol) compared with dimer2 (-101.50 and -79.533 kcal/mol) based on both MM-PBSA and MM-GBSA methods, respectively. The difference in binding free energy is mostly due to the fact that the interfacial region is rich in flexible loops, whose extents are different in both the dimers. [Color figure can be viewed in the online issue, which is available at wileyonlinelibrary.com.]

package. All the docked complexes were subjected to three rounds of minimization followed by heating, density equilibration and pressure equilibration. The equilibrated structure was then MD simulated for 10 ns. Similar methods, parameters and the constraints were used as described above for the MD simulation of GCP4 and γ-tubulin complex. The structures were recoreded every 1 ps resulting in a trajectory with 10,000 frames.

Calculation of binding free energy of docked complexes

The calculation of binding free energy between the ligands and the complex of GCP4 and γ-tubulin was carried out using the MM-GBSA and MM-PBSA method. Similar scoring sheme was used for the calculation of binding free energy as described above between GCP4 and γ-tubulin. Binding free energy of ligands with the complex of GCP4 and γ-tubulin was calculated as the ensemble average of the binding free energy from a total of 500 snapshots, extracted every 10 ps from the last 5 ns of simulation out of 10 ns of MD run.

Decomposition of ligand-residue interaction of docked complexes

The energy contribution of each residue in docked complex was estimated using the MM-GBSA decomposition process in Amber 11.0 over the 500 frames obtained every 10 ps from the last 5 ns of simulation out of 10 ns of MD run. The binding free energy of each ligand-residue pair includes three energy terms: the van der Waals contribution (ΔE_{vdw}), the electrostatic contribution (ΔE_{ele}) and the solvation contribution (ΔE_{sol}). All the energy components are calculated using the same frames obtained from MD trajectories that were used for calculation of binding free energy of ligands with the complex of GCP4 and γ-tubulin.

RESULTS AND DISCUSSIONS

Structural stabilities of the complex of GCP4 and γ-tubulin from MD simulations

The complexes (dimer1 and dimer2) of GCP4 and γ-tubulin were simulated for 25 ns to monitor the stability of the system during a long run of MD simulation. The equilibration of the MD trajectories was monitored based on the convergence of plots of root mean square deviations (RMSD) of Cα carbon atoms. As can be seen from Figure 2(A), the relative fluctuation in the RMSD of Cα carbon atoms (Cα-rmsd) is very small after equilibration 5 ns of simulation. The overall RMSD ranges from 0 to 3.5 Å. Furthermore, root mean square fluctuations (RMSF) of Cα-atoms were also calculated for both dimer1 and dimer2 to find any changes in the residue flexibilities. The RMSF values were plotted against residue numbers as shown in Figure 2(B). The

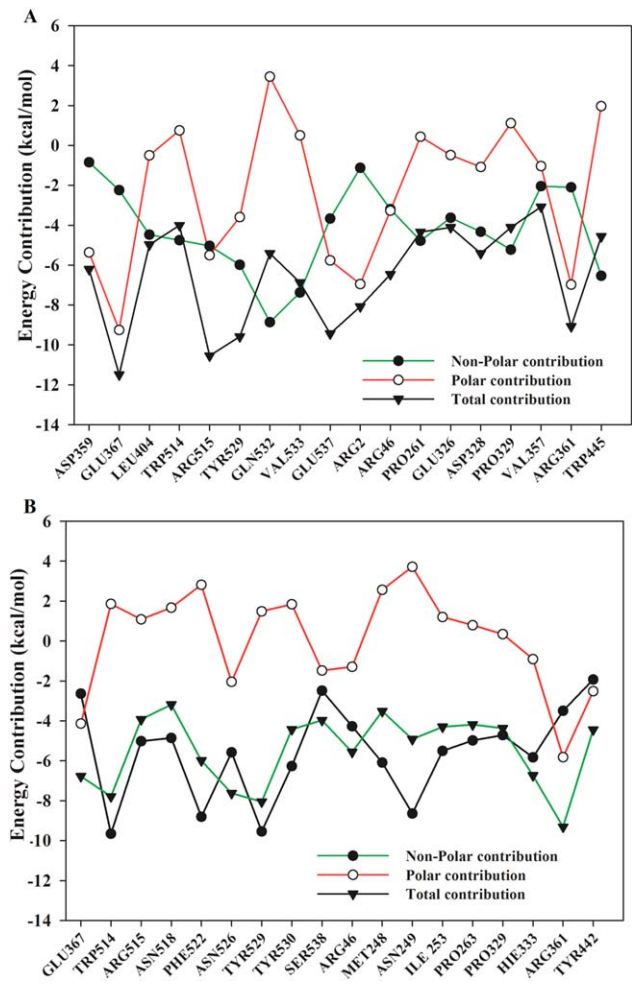

Figure 5

Polar and nonpolar energy contribution of hotspot residues. The decomposition of total energy contributions into polar and nonpolar energy components of hotspot amino acids in the binding process of GCP4 and γ-tubulin in dimer1 (**A**) and dimer2 (**B**). For both GCP4 and γ-tubulin the hotspot amino acids make considerable nonpolar solvation contributions compared with the polar contributions. Polar interactions were calculated as sum of electrostatic ($\Delta E_{i,ele}$) and polar solvation ($\Delta G_{i,sol,GB}$) energy components while the nonpolar interactions were calculated as sum of van der waals ($\Delta E_{i,vdw}$) and nonpolar solvation component ($\Delta G_{i,sol\text{-}np}$). [Color figure can be viewed in the online issue, which is available at wileyonlinelibrary.com.]

Table III

$\Delta\Delta G_{bind}$ for Hotspot Amino Acids

Chain	Residue	$\Delta\Delta G_{bind}$ (MM-GBSA)	$\Delta\Delta G_{bind}$ (MM-PBSA)
(a) Dimer1			
GCP4 (Chain A)	ASP359	12.32	28.02
	GLU367	32.62	40.53
	LEU404	3.09	2.18
	TRP514	6.28	6.04
	ARG515	15.54	14.60
	TYR529	6.45	3.34
	GLN532	5.26	7.62
	VAL533	3.84	5.25
	GLU537	19.69	23.41
γ-Tubulin (Chain B)	ARG2	16.98	31.94
	ARG46	17.05	27.51
	PRO261	1.68	1.41
	GLU326	2.97	4.31
	ASP328	21.10	22.04
	PRO329	2.98	1.21
	VAL357	.51	0.81
	ARG361	16.23	16.25
	TRP445	2.51	1.62
(b) Dimer2			
GCP4 (Chain A)	GLU367	17.01	24.21
	TRP514	11.01	10.12
	ARG515	9.15	10.67
	ASN518	5.26	4.56
	PHE522	8.48	4.82
	ASN526	6.85	6.15
	TYR529	11.56	8.45
	TYR530	9.48	2.95
	SER538	4.76	5.12
γ-Tubulin (Chain B)	ARG46	10.41	12.33
	MET248	5.51	7.03
	ASN249	4.26	9.64
	ILE 253	2.82	0.95
	PRO263	2.23	3.41
	PRO329	3.82	5.95
	HIS333	10.16	8.86
	ARG361	9.12	10.47
	TYR442	3.78	1.93

Computational alanine scanning mutagenesis was carried for all the 36 hotspot amino acids between GCP4 and γ-tubulin for both dimer1 and dimer2. Those amino acid residues, which contributed < -3 kcal/mol to the binding free energy of GCP4 and γ-tubulin complex, were mutated to alanine, one by one, to determine $\Delta\Delta G_{bind}$. $\Delta\Delta G_{bind}$ was calculated as $\Delta G_{mutant} - \Delta G_{wild\ type}$.

residues with higher RMSF tend to show more flexibility. From the structural analysis, we can see that both the complexes are stable during the monitored MD simulation.

Analysis of calculated binding free energy between GCP4 and γ-tubulin

The binding free energies and their components between GCP4 and γ-tubulin were calculated independently for both dimer1 and dimer2 and presented in Table I. We have considered last 500 frames from the last 5 ns of trajectory out of 25 ns MD simulation run to calculate the ensemble average of the free energy of binding using both MM-GBSA and MM-PBSA methods. The results obtained from both the methods suggested very robust interactions between the GCP4 and γ-tubulin, essentially driven by the nonpolar forces. The mean values of the binding free energies (ΔG_{bind}) based on MM-GBSA method are −170.19 and −101.50 kcal/mol, respectively, for both dimer1 and dimer2. In contrary the ΔG_{bind} based on MM-PBSA are estimated to be −158.82 kcal/mol for dimer1 and −79.533 kcal/mol for dimer2. Hence, there is a difference of 11.37 kcal/mol for dimer1 and 21.97 kcal/mol for dimer2 between the two methods. This derives from the difference in calculation of the contribution to the polar solvation energy, which is

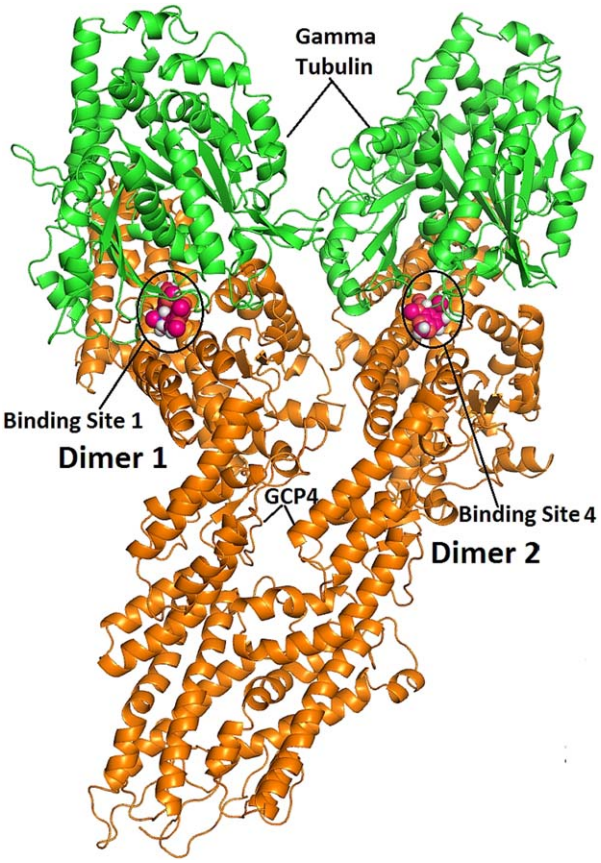

Figure 6

Predicted binding sites. γ-tubulin-GCP4 tetramer showing noscapinoid binding site 1 and binding site 2. Both the binding sites, marked as spheres, lie at the interface of γ-tubulin-GCP4 complex. [Color figure can be viewed in the online issue, which is available at wileyonlinelibrary.com.]

higher in the MM-PBSA calculation (201.11 and 19.601 kcal/mol) compared with MM-GBSA (189.74 and −2.364 kcal/mol) among both the dimers. Similarly the net difference in binding free energy between dimer1 and dimer2 of GCP4 and γ-tubulin complex was mostly due to the fact that the interfacial region is rich in flexible loops, whose extents are different in both the dimers. Very robust van der Waals (ΔE_{VDW}) interactions, to the magnitude of −259.46 and −195.71 kcal/mol were observed for dimer1 and dimer2, respectively. The net polar component [$\Delta G_{(ele,\ PB/GB)} = \Delta E_{ele} + \Delta G_{(PB/GB)}$] was observed to be unfavourable in the interaction between GCP4 and γ-tubulin among both the dimers (Table I). The unfavorable polar contributions were observed to overcome with highly favorable nonpolar components ($\Delta E_{vdw} + \Delta G_{sol\text{-}np}$) among both the dimers. Interactions between GCP4 and γ-tubulin seem to be steered by nonpolar component. This can be explained by the tendency of the nonpolar residues to readily bury themselves in the hydrophobic pockets and displace water.

Table IV
Glide Docking Scores

Ligand	Glide e_{vdw}	Glide e_{coul}	Glide Emodel	Glide energy	XP_{GScore}
A: Site 1					
Noscapine	−22.72	−4.34	−31.95	−27.06	−7.59
Amino	−9.18	−4.95	40.25	−14.13	−7.56
Bromo	−26.88	−5.67	−44.30	−32.55	−9.08
NM87	−23.46	−2.68	−31.04	−26.13	−6.74
NM372	−37.18	−10.93	−69.51	−48.11	−7.28
B: Site 2					
Noscapine	−38.25	−8.17	−53.86	−46.41	−6.83
Amino	−27.64	−11.70	−51.58	−39.34	−6.73
Bromo	−38.84	−10.11	−47.14	−48.95	−9.19
NM87	−24.69	−4.28	−36.71	−28.97	−6.66
NM372	−36.61	−7.20	−63.52	−43.82	−7.70

After predicting the binding sites, extra-precision docking was performed using Glide XP dock protocol implemented in Schrodinger package. XP_{Gscore} (kcal/mol) of noscapenoids (noscapine, amino-noscapine, bromo-noscapine) and the reference compounds (NM87 and NM372) with GCP4 and γ-tubulin heterodimer are presented in the table. Noscapinoids showed better docking score compared to the reference molecules, NM87 and NM372.

Per residue energy contribution to the binding free energy

Energy contribution of each residue in the γ-tubulin-GCP4 complex among both dimer1 and dimer2 was calculated using the MM-GBSA method to investigate the details of protein-protein interactions at the atomic level and plotted in Figure 3. In contrast, the decomposition of binding free energy calculated on the basis of MM-PBSA into per residue basis was not so far possble because PB nonpolar solvation energies are currently not decomposable using Amber simulation package. Similar studies have been reported earlier in the insulin dimer,[53] TCR-p-MHC,[54] Ras-Raf, and Ras-RalGDS[55] complexes and γ-γ tubulin dimers.[56] The results from these studies demonstrated good correlations between the calculated per residue binding free energy and the experimental binding free energies differences for the alanine mutants. Toward this end the predictive binding energy ($\Delta G_{bind,GB}$) between GCP4 and γ-tubulin was decomposed into contributions from the residues of the two partners. We identified 18 hotspot amino acids that have the highest impact (per residue contribution <-3 kcal/mol) on the GCP4 and γ-tubulin interaction (Fig. 3). The detailed energy components are included in Table II and the spatial distributions of these hotspots at the binding interface between GCP4 and γ-tubulin are shown in Figure 4 for both the dimers. As shown in Figure 3(A), for dimer1, seven amino acids (Asp359, Glu367, Arg515, Tyr529, Glu537, Gln532, and Val533) on the surface of GCP4 and five amino acids (Arg2, Arg46, Pro329, Arg361, and Trp445) on the surface of γ-tubulin make greater contributions to the binding of GCP4 and γ-tubulin, each yielding <-5 kcal/mol of binding free energy. In addition, two amino acids (Leu404 and Trp514) from GCP4 and four amino acids (Pro261, Glu326, Asp328, and Val357) from γ-tubulin have

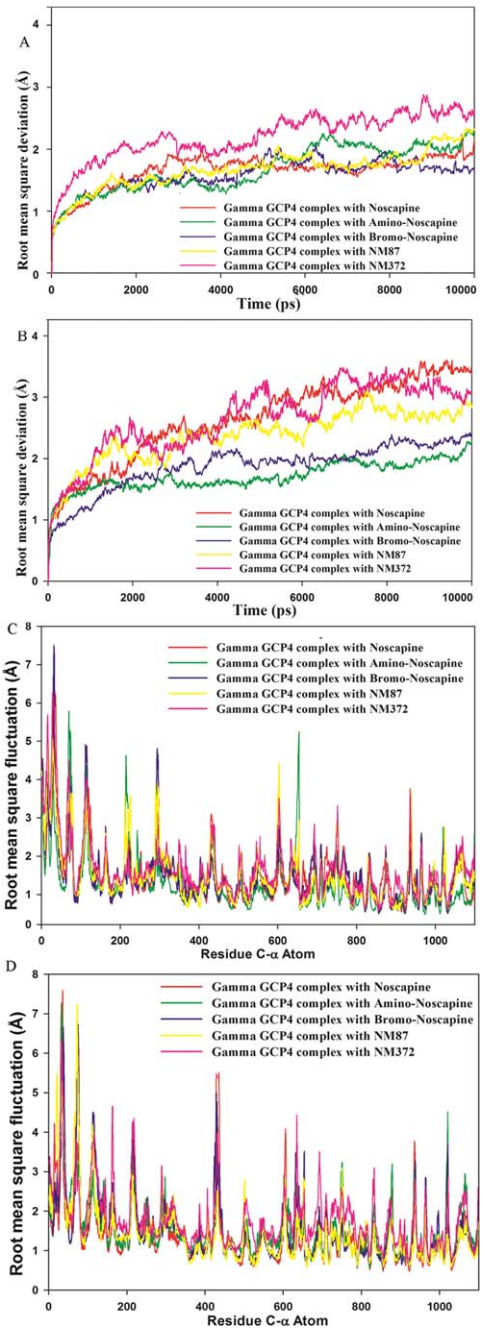

Figure 7

Root mean square daviation (RMSD) and root mean square fluctuation (RMSF) of Cα atoms of GCP4 and γ-tubulin complex in the bound form with ligands. The root mean square deviations (RMSD) of Cα atoms in dimer1 (**A**) and dimer2 (**B**) in the bound form with different ligands (noscapine, amino-noscapine, bromo-noscapine, NM87, and NM372) during the entire duration of MD simulation. The relative fluctuation in the RMSD of the Cα atoms is very small after 4000 ps, revealed that each system reaches equilibrium at 4000 ps. RMSF of residues in the complex of GCP4 and γ-tubulin in dimer1 (**C**) and dimer2 (**D**) in the bound form with different ligands (noscapine, amino-noscapine, bromo-noscapine, NM87, and NM372) during the entire duration of MD simulation. The residues with higher RMSF tend to show more flexibility. [Color figure can be viewed in the online issue, which is available at wileyonlinelibrary.com.]

considerable energy contributions to the binding process of GCP4 and γ-tubulin, each yielding between −3 and −5 kcal/mol of free energy. Contrastingly for dimer2 albite different amino acids shown to contribute in the interaction betwen GCP4 and γ-tubulin. As shown in Figure 3(B), five residues (Glu367, Trp514, Phe522, Tyr529, and Asn526) on the surface of GCP4 and three amino acids (Arg46, His333, Arg361) on the surface of γ-tubulin make larger contribution of <-5 kcal/mol each in the binding process. In addition, four amino acids (Arg515, Asn518, Tyr530, and Ser538) of GCP4 and six amino acids (Met248, Asn249, Ile253, Pro263, Pro329, and Arg442) of γ-tubulin contributed binding free energy of −3 to −5 kcal/mol in the binding process. The mismatches in some of the hotspot amino acids between both the dimer is due to the fact that the interfacial region is rich in flexible loops, whose extents are different in both the dimers. For example, examination of the structure of the two contact regions reveals that the helix composed of 15 residues (328 − 342) in dimer2, whereas only 8 residues long (335 − 342) in dimer1. However, all the predicted hotspots between both the dimers were observed to lie at the interface of γ-tubulin-GCP4 complex (Fig. 4). Furthermore, to determine the detailed contribution of each hotspot amino acids, the total binding free energy was further decomposed into various energy components like van der Waals, electrostatic, polar salvation, and nonpolar solvation (Table III). The results reveals that most of the important amino acids for both GCP4 and γ-tubulin make considerable van der Waals and nonpolar solvation contributions compared with the polar contributions (Fig. 5).

To further verify the individual contribution of the hotspot amino acids identified above to binding free energy between GCP4 and γ-tubulin interactions we performed computational alanine scanning. The method proposes to mutate the amino acids of interest, one by one to alanine and recalculate the binding free energy of the mutant using MM-PBSA and MM-GBSA methods and compared with the wild type. It also reveals that a minute local change in the protein does not affect the overall conformation of the protein-protein complex. The results of the computational alanine scanning of the amino acids contributed significantly in the interaction of GCP4 and γ-tubulin is included in Table III. The results obtained by the decomposition of the binding energy and computational alanine scanning were found to be quite consistent and this indicates the reliability of our analysis. After performing computational alanine scanning for hotspots, a substantial decrease in the binding free energy was observed. The mutation to alanine led to a decrease in binding energy for each hotspot amino acid at least by 0.51 kcal/mol in dimer1 and 2.23 kcal/mol in dimer2 using the MM-GBSA method, while by using the MM-PBSA method

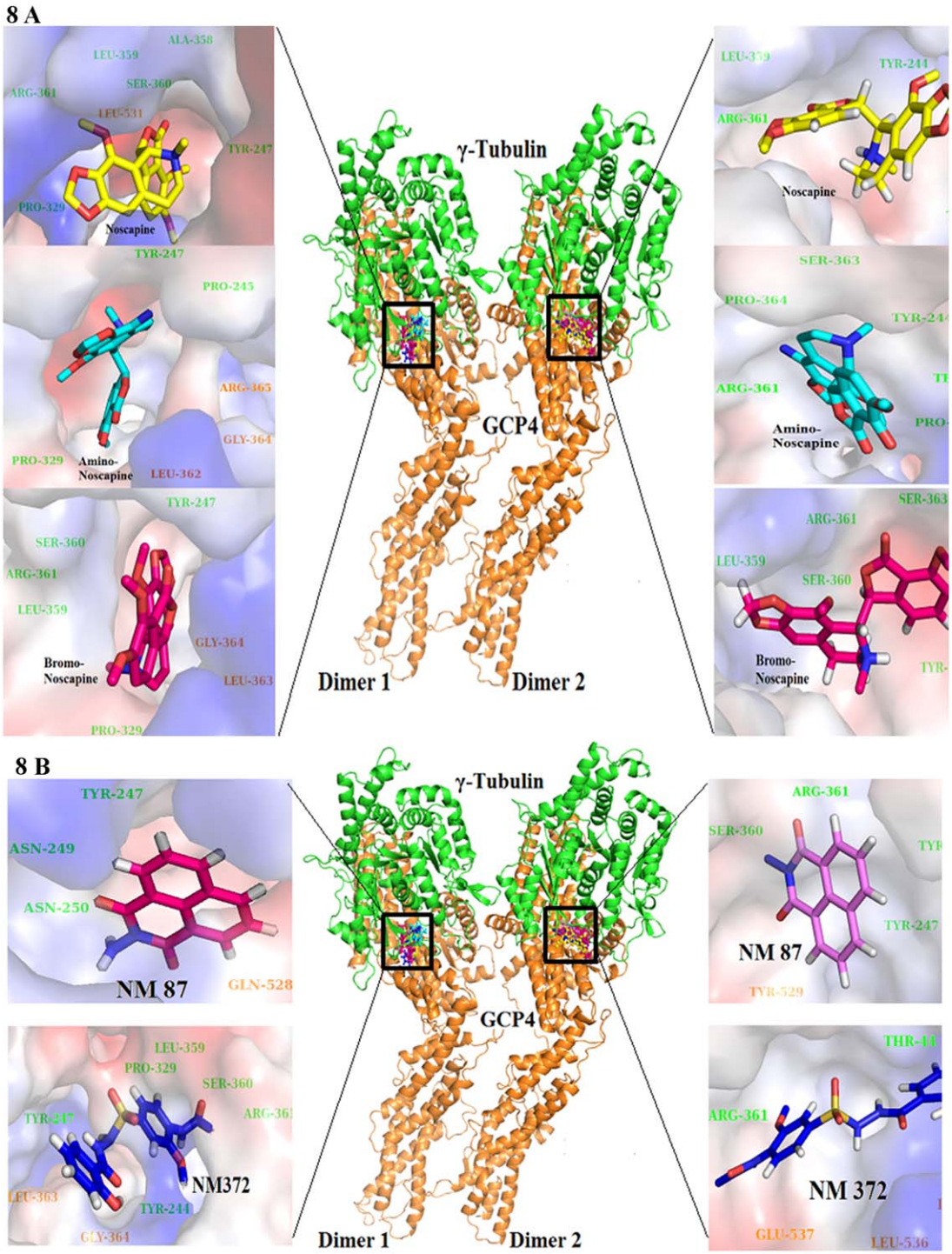

Figure 8

Binding modes of noscapinoids. **A**: Noscapinoids (Noscapine, Amino-Noscapine, and Bromo-Noscapine) docked into dimer1 and dimer2. The zoomed views show the binding modes of the noscapinoids alone. The residues that show contribution of more than 1 kcal/mol to the binding affinity are labeled green for γ-tubulin and orange for GCP4. Binding modes of Reference molecules. **B**: Both the reference molecules (NM 87 and NM 372) docked into dimer1 and dimer2. The zoomed views show the binding modes of the reference molecules. The residues that show contribution of more than 1 kcal/mol to the binding affinity are labeled green for γ-tubulin and orange for GCP4.

the minimum drop in binding free energy was 0.81 kcal/mol in dimer1 and 0.95 kcal/mol in dimer2, thereby reducing the strength of γ-tubulin-GCP4 interaction. This reiterates that the hotspot amino acids identified in the interaction between γ-tubulin-GCP4 are very crucial.

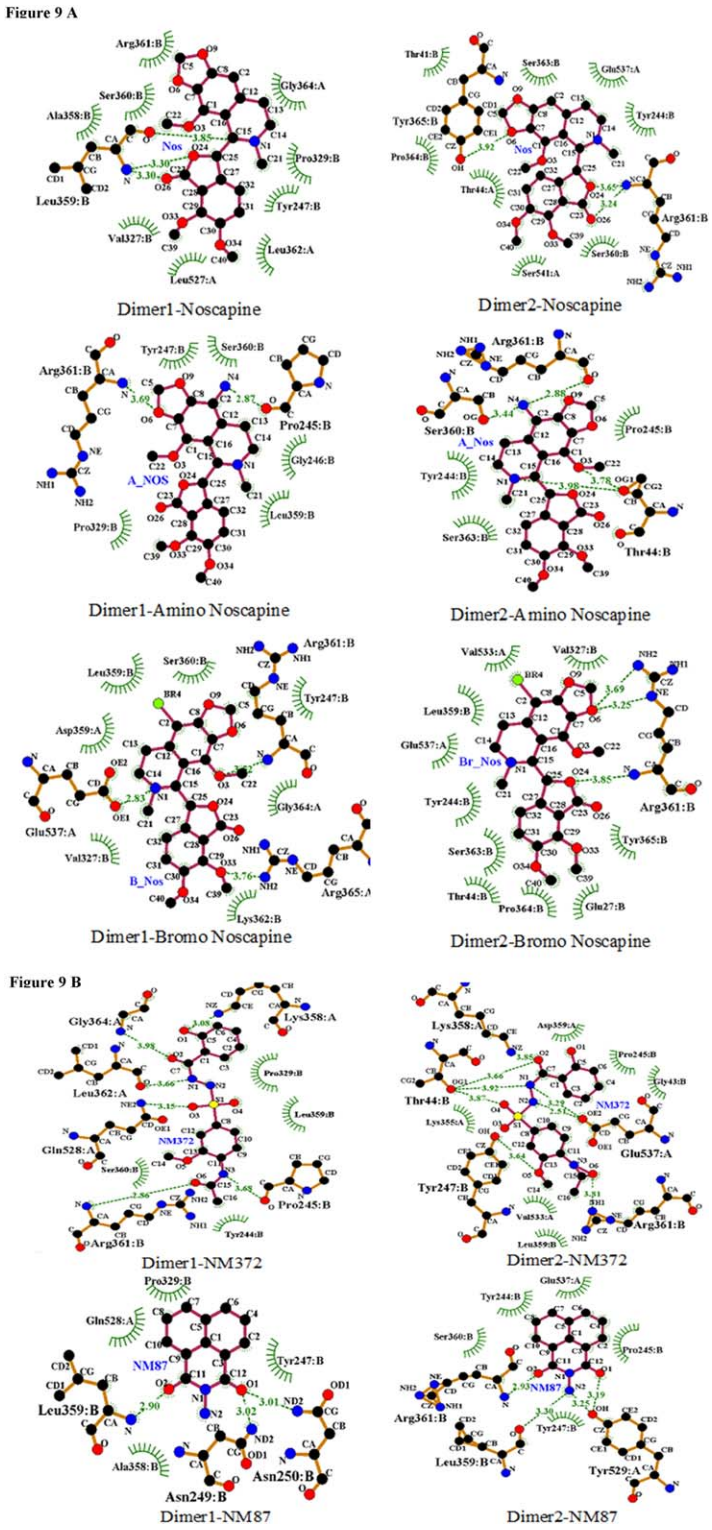

Figure 9

2-D ligplot of noscapinoids. **A:** A 2-D representation of the binding mode of noscapinoids (Noscapine, Amino-Noscapine, and Bromo-Noscapine) with the complex of GCP4 and γ-tubulin. In the images "A" denotes the residues of GCP4 and "B" denotes the residues of γ-tubulin. 2-D ligplot of reference molecules. **B**: A 2-D representation of the binding mode of reference compounds (NM87 and NM372) with the complex of GCP4 and γ-tubulin. In the images "A" denotes the residues of GCP4 and "B" denotes the residues of γ-tubulin. [Color figure can be viewed in the online issue, which is available at wileyonlinelibrary.com.]

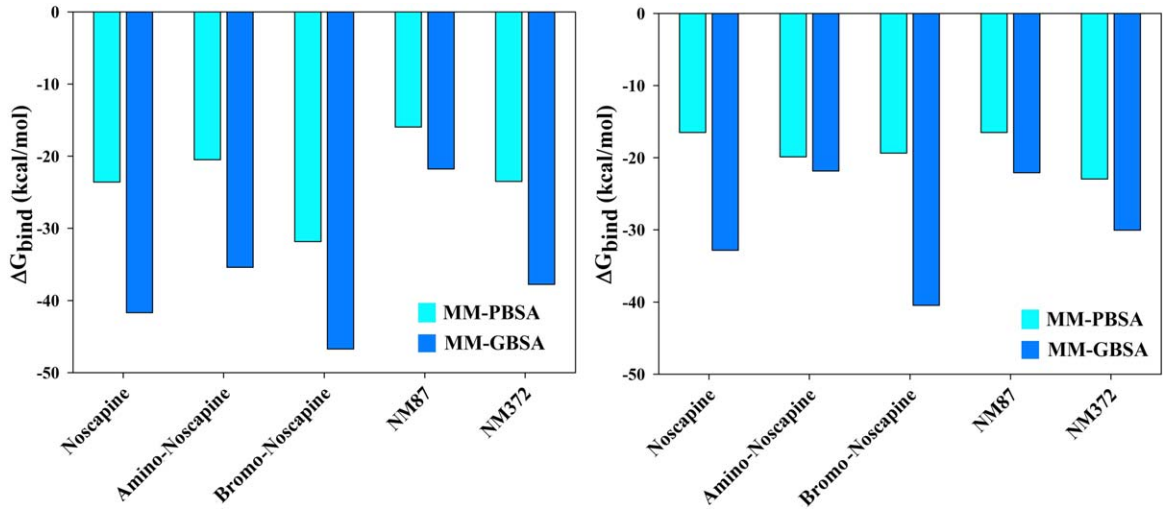

Figure 10

Calculated binding free energy of compounds 1 − 5. The calculated binding free energy for each of the compounds; Noscapine, Amino-Noscapine, Bromo-Noscapine, and the reference molecules NM87 and NM372 with (**A**) dimer1 and (**B**) dimer2 of GCP4 and γ-tubulin using MM-PBSA and MM_GBSA methods. The noscapinoids showed improved in binding free energy compared to the previously reported both the reference compounds, indicate the possibility of binding of noscapinoids at the interface of GCP4 and γ-tubulin. [Color figure can be viewed in the online issue, which is available at wileyonlinelibrary.com.]

Interaction of compounds 1–5 with the complex of GCP4 and γ-tubulin

Molecular docking

We have adapted blind docking approach to predict the probable site of interaction of noscapinoids (noscapine, amino-noscapine, and bromo-noscapine that were reported to have anticancer activities) with the GCP4 and γ-tubulin complex in the absence of cocrystal structure. In this approach, we initially predicted all the binding sites of GCP4 and γ-tubulin complex, which consists of at least 5 site points per reported site using sitemap program of Schrodinger package for molecular docking evaluation of binding sites. All these sites along with their various physicochemical properties are included in Supporting Information Table S1. The probable site of interaction of noscapinoids onto GCP4 and γ-tubulin complex was screened out based on docking score. As mentioned in Supporting Information Table S2, all the molecules **1–5** shown better docking score with site 1 (belongs to dimer1) and site 2 (belongs to dimer2) were selected. The spatial localization of both site 1 and site 2 in the GCP4 and γ-tubulin complex is represented in Figure 6. As shown in figure, both the sites are located at the γ-tubulin surface that is juxtaposed wth its binding interface with GCP4. Eventually, both the binding sites turned out to be consistent with the experimentally determined binding site reported previously by Cala *et al.* (2013).[19] Cala *et al.* also screened 20 molecules and experimentally tested their binding affinity. We used two molecules from this study, NM87 and NM372 as reference, along with three noscapinoids and docked into both the binding sites in a single experiment. Surprisingly, all the noscapinoids showed better docking scores compared with the reference molecules (Table IV), demonstrating the possibility of interactions of noscapinoids at the interface of GCP4 and γ-tubulin complex. Molecular docking methods are widely used by pharmaceutical industries to study drug-target interactions to understand the basic electronic/steric features required for therapeutic action and to design new drug candidates with improved activities. These docking calculations provide insight into interactions of noscaponoids with the GCP4 and γ-tubulin complex.

Determination of binding mode of compounds 1–5 with GCP4 and γ-tubulin complex

Although computationally demanding, we determined the preferential binding mode of compounds **1-5** at the interface of GCP4 and γ-tubulin complex by MD simulations. Toward this end the complexes obtained after molecular docking were simulated for 10 ns to obtain a total of 10,000 frames. The stability of the system was monitored by means of RMSD of Cα-atoms during the entire duration of simulation as shown in Figure 7(A,B) for both the dimers. The RMSD of all the complexes reaches equilibrium at 4000 ps and after that the RMSDs of atoms oscillated between 2-4 Å. Furthermore, the local protein mobility was analysed by calculating the time averaged RMSF values in free and bound form of GCP4 and γ-tubulin complexes with compounds **1–5**. The RMSF values were plotted against residue numbers based

on the 10,000 ps trajectory as shown in Figure 7(C,D) for both the dimers. The profiles of atomic fluctuations were found to be very similar for all the compounds **1–5**. The compounds **1–5** were observed to dock into the GCP4 and γ-tubulin complex throughout the 10 ns simulation. Specifically the MD simulation makes an important contribution to understand the effect of binding of compounds **1–5** on conformational changes of GCP4 and γ-tubulin complex and the stability of protein-ligand system in aqueous solution. The average structure of docked complexes of compounds **1–5** with γ-tubulin-GCP4 complex was generated out of 500 frames obtained every 10 ps from the last 5 ns of MD trajectory and was used to elucidate the binding mode and ligplot analysis. The binding mode of **1–5** involves interactions of the compounds with both GCP4 and γ-tubulin at sites reported earlier[20] and are well accomodated inside the binding cavity [Fig. 8(A,B)]. The binding mode of ligands with the protein complex was represented in two steps: (a) receptor residues that have strong interactions with the ligand, such as a favourable hydrogen-bonding interactions, and (b) receptor residues that are close to the ligand, but whose interactions with the ligand are weak or diffuse, such as hydrophobic interaction. The differential mode of interactions of compounds **1–5** with the residues of GCP4 and γ-tubulin complex are represented in the Ligplot [Fig. 9(A,B)]. As seen in the figure several hydrogen bonds and hydrophobic interactions are involved in their binding.

Table V
Binding Free Energy

Contribution	Noscapine	Amino-Noscapine	Bromo-Noscapine	NM87	NM372
(a) Dimer1					
ΔE_{INT}	0.00	0.00	0.00	0.00	0.00
ΔE_{VDW}	−52.03	−48.94	−55.48	V24.84	−51.34
ΔE_{ELE}	−220.92	−204.21	−236.13	−18.49	−39.05
$\Delta E_{GAS/\Delta E\ MM}$	−272.94	−253.12	−291.60	−43.33	2.00
ΔG_{PB}	253.49	236.72	263.75	29.04	70.75
$\Delta G_{SOL\text{-}NP}$	−4.15	−4.09	−3.99	−1.67	−3.86
$\Delta G_{SOLV,PB}$	249.35	232.62	259.77	27.37	66.90
$\Delta G_{ELE,PB}$	32.57	32.51	27.62	10.56	31.71
$\Delta G_{bind,PB}$	−23.60	−20.50	−31.83	−15.95	−23.50
G_{GB}	236.89	223.22	250.54	24.71	59.03
$G_{SOLV,GB}$	231.25	217.73	244.87	21.56	52.63
$G_{ELE\ GB}$	15.97	19.01	14.41	6.22	19.98
$\Delta G_{bind,\ GB}$	−41.69	−35.40	−46.73	−21.76	−37.76
ΔE_{INT}	0.00	0.00	0.00	0.00	0.00
ΔE_{VDW}	−46.95	−34.61	−52.03	−29.52	−40.22
ΔE_{ELE}	−226.88	−230.12	−234.78	−19.60	−27.18
$\Delta E_{GAS/\Delta E\ MM}$	−273.81	−264.70	−286.80	−49.12	−67.40
ΔG_{PB}	261.34	247.50	271.30	34.56	48.28
ΔG_{SOL-NP}	−4.02	−2.67	−3.88	−1.92	−3.84
$\Delta G_{SOLV,PB}$	257.32	244.83	267.43	32.64	44.44
$\Delta G_{ELE,PB}$	34.46	17.38	36.52	14.95	21.10
$\Delta G_{bind,PB}$	−16.50	−19.87	−19.37	−16.49	−22.96
G_{GB}	246.27	246.38	251.66	30.49	42.92
$G_{SOLV,GB}$	241.00	242.87	246.35	27.06	37.36
$G_{ELE\ GB}$	19.39	16.26	16.88	10.89	15.75
$\Delta G_{bind,\ GB}$	−32.82	−21.84	−40.45	−22.07	−30.04

Binding affinity of drugs with GCP4 and γ-tubulin complex was calculated using MM-GBSA/MM-PBSA methods. Binding free energy (kcal/mol) and the respective energy components of compounds **1−5** binding to GCP4 and γ-tubulin dimers are given in the table below.

Binding free energy of compounds 1–5 with the complex of GCP4 and γ-tubulin

Binding free energies of noscapinoids (noscapine, amino-noscapine, and bromo-noscapine) and the reference molecules (NM372 and NM87) with dimer1 and dimer2 of GCP4 and γ-tubulin were calculated using the MM-PBSA and MM-GBSA approach. The predictive binding free energy comes out to be even better for the noscapinoids compared with the reference molecules based on both MM-GBSA and MM-PBSA methods (Fig. 10). The binding free energy of compounds **1–5** and the respective energy components are include in Table V. For all complexes, the binding energy was decomposed into its various energy components (the electrostatic, van der Waals and solvation). Both van der Waals (ΔE_{VDW}) and the electrostatic component (ΔE_{ELE}) were observed to make very significant contributions to the free energy of binding. However, the net polar contribution [$\Delta G_{(ele,PB/GB)} = \Delta E_{ele} + \Delta G_{(PB/GB)}$] was rendered unfavorable due to very large penalty imposed by the desolvation component ($\Delta G_{PB/GB}$) while the net nonpolar component (ΔE_{vdw}) and ($\Delta G_{sol\text{-}np}$) were observed to make highly favourable contribution to the binding free energy (Fig. 11). On analyzing the energy contribution of each residue in the complex, Tyr247 and Arg361 of γ- tubulin were observed to make significant contribution to the binding of ligands for all the complexes. Ligplot analysis also illustrates strong interaction of Arg361 of γ-tubulin with all the three drug molecules in both the complexes, mostly through H-bond formation (Fig. 9). It is our hope that the results presented here provide new grounds for further investigations of the therapeutic potential of noscapinoids against microtubule-nucleating γ-tubulin complexes.

CONCLUSION

This computational study provides insights into the interactions between GCP4 and γ-tubulin in two different conformations using MD to calculate the binding free energy of binding in solvation and identifying key residues participating in the interactions. Further the complexes were subjected to molecular docking with potential anticancer drug, noscapinoid and two of its derivatives amino-noscapine and bromo-noscapine. The binding modes of the three noscapinoids with the GCP4 and γ-tubulin dimers were further illustrated using MD simulation and binding free energy calculations. All three drugs lodged themselves in the pockets located very close

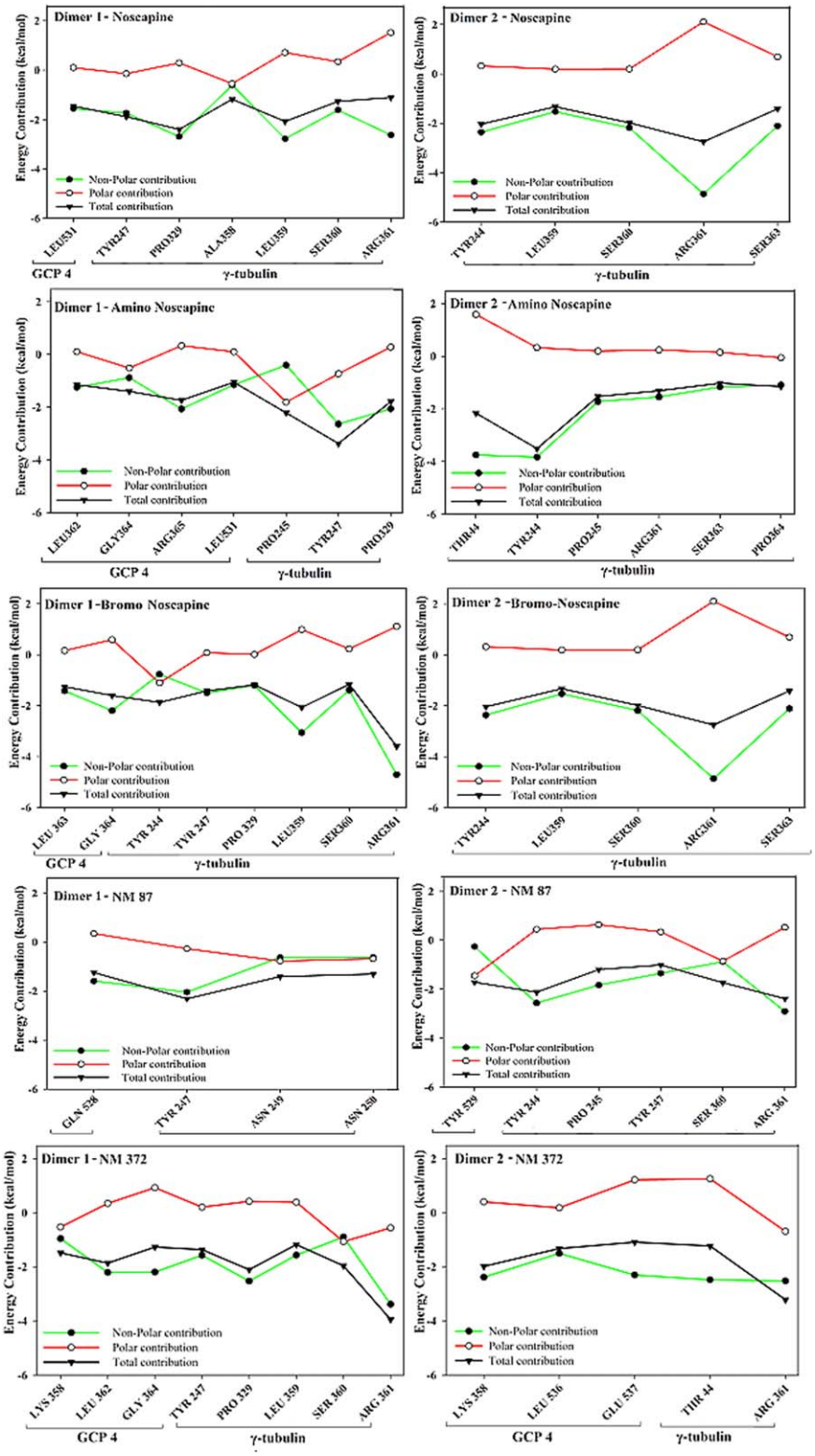

Figure 11

Energy contributions of hotspot amino acids. Nonpolar, polar as well as total energy contributions of the amino acid residues that contribute most to the stability of the protein ligand complex. Polar interactions were calculated as sum of electrostatic ($\Delta E_{i,ele}$) and polar solvation ($\Delta G_{i,sol,GB}$) energy components while the nonpolar interactions were calculated as sum of van der Waals ($\Delta E_{i,vdw}$) and nonpolar solvation component ($\Delta G_{i,sol\text{-}np}$). [Color figure can be viewed in the online issue, which is available at wileyonlinelibrary.com.]

to the binding interface of the GCP4 and γ-tubulin. The molecular interaction of all the three drugs are leveraged more toward γ-tubulin. The binding modes of noscapine and bromo-noscapine are quite similar with both the drugs showing strong interaction with Tyr247, Pro329, Leu359, Ser360, and Arg361 of γ-tubulin in dimer1. Both drugs also displayed similar interactions with Tyr244, Leu359, and Arg361 in dimer2. Pro329 and Arg361 are also two important identified hotspot amino acids in the interaction of GCP4 and γ-tubulin. We also observe that in almost all complexes the drug makes H-bond with Arg361. Therefore, if these drugs can interfere with a subset of the hotspot amino acids they might be able to perturb some of the interactions between GCP4 and γ-tubulin and further destabilize the γTuRC. Nevertheless, our results offer noscapinoids an important possible chemical framework for the further design of more potent compounds.

ACKNOWLEDGMENT

The authors are thankful to Dr. Georges Czaplicki, from the Université de Toulouse, UPS, Toulouse, France, for providing the structure file consisting of atomic coordinates of the GCP4 and γ-tubulin tetramer. The authors are thankful to Prof. B. Jayaram and the staff of the SCFBio laboratory at IIT-Delhi for providing the access to their supercomputing facility to perform MD simulation. They are greatly indebted to the anonymous reviewers of this manuscript for their helpful suggestions.

REFERENCES

1. Lecland N, Lüders J. The dynamics of microtubule minus ends in the human mitotic spindle. Nat Cell Biol 2014;16:770–778.
2. Oakley BR, Oakley CE, Yoon Y, Jung MK. γ-Tubulin is a component of the spindle pole body that is essential for microtubule function in Aspergillus nidulans. Cell 1990;61:1289–1301.
3. Zheng Y, Jung MK, Oakley BR. γ-Tubulin is present in Drosophila melanogaster and Homo sapiens and is associated with the centrosome. Cell 1991;65:817–823.
4. Stearns T, Evans L, Kirschner M. γ-Tubulin is a highly conserved component of the centrosome. Cell 1991;65:825–836.
5. Horio T, Uzawa S, Jung MK, Oakley BR, Tanaka K, Yanagida M. The fission yeast gamma-tubulin is essential for mitosis and is localized at microtubule organizing centers. J Cell Sci 1991;99:693–700.
6. Joshi HC, Palacios MJ, McNamara L, Cleveland DW. γ-Tubulin is a centrosomal protein required for cell cycle-dependent microtubule nucleation. Nature 1992;365:80–83.
7. Joshi HC. γ-Tubulin: The hub of cellular microtubule assemblies. Bioessays 1993;15:637–643.
8. Oegema K, Wiese C, Martin OC, Milligan RA, Iwamatsu A, Mitchison TJ, Zheng Y. Characterization of two related Drosophila γ-tubulin complexes that differ in their ability to nucleate microtubules. J Cell Biol 1999;144:721–733.
9. Guillet V, Knibiehler M, Gregory-Pauron L, Remy MH, Chemin C, Raynaud-Messina B, Agard DA, Bon C, Kollman JM, Merdes A, Mourey L. Crystal structure of gamma-tubulin complex protein GCP4 provides insight into microtubule nucleation. Nat Struct Mol Biol 2011;18:915–919.
10. Kollman JM, Zelter A, Muller EG, Fox B, Rice LM, Davis TN, Agard DA. The structure of the gamma-tubulin small complex: implications of its architecture and flexibility for microtubule nucleation. Mol Biol Cell 2008;19:207–215.
11. Cala O, Remy MH, Guillet V, Merdes A, Mourey L, Milon A, Czaplicki G. Virtual and biophysical screening targeting the γ-tubulin complex–a new target for the inhibition of microtubule nucleation. PLoS One 2013;8:e63908. doi: 10.1371/journal.-pone.0063908. Print 2013.
12. Joshi HC, Palacios MJ, McNamara L, Cleveland DW. Gamma-tubulin is a centrosomal protein required for cell cycle-dependent microtubule nucleation. Nature 1992;356:80–83.
13. Raynaud-Messina B, Merdes A. g-Tubulin complexes and microtubule organization. Curr Opin Cell Biol 2007;19:24–30.
14. Niu Y, Liu T, Tse GM, Sun B, Niu R, Li HM, Wang H, Yang Y, Ye X, Wang Y, Yu Q, Zhang F. Increased expression of centrosomal a, g-tubulin in atypical ductal hyperplasia and carcinoma of the breast. Cancer Sci 2009;100:580–587.
15. Liu T, Niu Y, Yu Y, Liu Y, Zhang F. Increased g-tubulin expression and P16INK4A promoter methylation occur together in preinvasive lesions and carcinomas of the breast Ann Oncol. 2009;20:441–448.
16. Montero-Conde C, Martín-Campos JM, Lerma E, Gimenez G, Martínez-Guitarte JL, Combalía N, Montaner D, Matías-Guiu X, Dopazo J, de Leiva A, Robledo M, Mauricio D. Molecular profiling related to poor prognosis in thyroid carcinoma. Combining gene expression data and biological information. Oncogene 2007;27:1554–1561.
17. Li Y, Hussain M, Sarkar SH, Eliason J, Li R, Sarkar FH. Gene expression profiling revealed novel mechanism of action of Taxotere and Furtulon in prostate cancer cells. BMC Cancer 2005;5:7.
18. Orsetti B, Nugoli M, Cervera N, Lasorsa L, Chuchana P, Ursule L, Nguyen C, Redon R, du Manoir S, Rodriguez C, Theillet C. Genomic and expression profiling of chromosome 17 in breast cancer reveals complex patterns of alterations and novel candidate genes. Cancer Res 2004;64:6453–6460.
19. Katsetos CD, Reddy G, Dráberová E, Smejkalová B, Del Valle L, Ashraf Q, Tadevosyan A, Yelin K, Maraziotis T, Mishra OP, Mörk S, Legido A, Nissanov J, Baas PW, de Chadarévian JP, Dráber P. Altered cellular distribution and subcellular sorting of g-tubulin in diffuse astrocytic gliomas and human glioblastoma cell lines. J Neuropathol Exp Neurol 2006;65:465–477.
20. Cala O, Remy MH, Guillet V, Merdes A, Mourey L, Milon A, Czaplicki G. Virtual and biophysical screening targeting the γ-tubulin complex–a new target for the inhibition of microtubule nucleation. PLoS One 2013;8:e63908. doi: 10.1371/journal.pone.0063908.
21. Ravelli RB, Gigant B, Curmi PA, Jourdain I, Lachkar S, Sobel A, Knossow M. Insight into tubulin regulation from a complex with colchicine and a stathmin-like domain. Nature 2004;428:198–202.
22. Loöwe J, Li H, Downing KH, Nogales E. Refined structure of alpha beta-tubulin at 3.5 A resolution. J Mol Biol 2001;313:1045–1057.
23. Aldaz H, Rice LM, Stearns T, Agard DA. Insights into microtubule nucleation from the crystal structure of human gamma-tubulin. Nature 2005;435:523–527.
24. Alushin, Gregory M., Gabriel C. Lander, Elizabeth H. Kellogg, Rui Zhang, David Baker, Eva Nogales. High-resolution microtubule structures reveal the structural transitions in αβ-tubulin upon GTP hydrolysis. Cell 2014;157:1117–1129.
25. Friesen DE, Barakat KH, Semenchenko V, Perez-Pineiro R, Fenske BW, Mane J, Wishart DS, Tuszynski JA. Discovery of small molecule inhibitors that interact with gamma-tubulin. Chem Biol Drug Des 2012;79:639–652.
26. Ye K, Ke Y, Keshava N, Shanks J, Kapp JA, Tekmal RR, Petros J, Joshi HC. Opium alkaloid noscapine is an antitumor agent that arrests metaphase and induces apoptosis in dividing cells. Proc Natl Acad Sci USA 1998;95:1601–1606.
27. Naik PK, Chatterji BP, Vangapandu SN, Aneja R, Chandra R, Kanteveri S, Joshi HC. Rational design, synthesis and biological

evaluations of amino-noscapine: a high affinity tubulin-binding noscapinoid. J Comput Aided Mol Des 2011;25:443–454.
28. Zhou J, Panda D, Landen JW, Wilson L, Joshi HC. Minor alteration of microtubule dynamics causes loss of tension across kinetochore pairs and activates the spindle checkpoint. J Biol Chem 2002;277: 17200–17208.
29. Zhou J, Gupta K, Yao J, Ye K, Panda D, Giannakakou P, Joshi HC. Paclitaxel-resistant human ovarian cancer cells undergo c-Jun NH_2-terminal kinase-mediated apoptosis in response to noscapine. J Biol Chem 2002;277:39777–39785.
30. Aneja R, Asress S, Dhiman N, Awasthi A, Rida PCG, Arora AK, Zhou J, Glass JD, Joshi HC. Non-toxic melanoma therapy by a novel tubulin-binding agent. Intl J Cancer 2010;126:256–265.
31. Case DA, Cheatham TE, Darden T, Gohlke H, Luo R, Merz KM, Onufriev A, Simmerling C, Wang B, Woods RJ. The Amber biomolecular simulation programs. J Comput Chem 2005;26:1668–1688.
32. Pearlman DA, Case DA, Caldwell JW, Ross WS, Cheatham III TE, DeBolt S, Ferguson D, Seibel G, Kollman P. AMBER, a package of computer programs for applying molecular mechanics, normal mode analysis, molecular dynamics and free energy calculations to simulate the structural and energetic properties of molecules. Comput Phys Commun 1995;91:1-41.
33. Cornell WD, Cieplak P, Bayly CI, Gould IR, Merz KM, Ferguson DM, Spellmeyer DC, Fox T, Caldwell JW, Kollman PA. A second generation force field for the simulation of proteins, nucleic acids, and organic molecules. J Am Chem Soc 1995;117:5179–5197.
34. Hornak V, Abel R, Okur A, Strockbine B, Roitberg A, Simmerling C. Comparison of multiple Amber force fields and development of improved protein backbone parameters. Proteins 2006;65:712–725.
35. Jorgensen WL, Chandrasekhar J, Madura JD, Impey RW, Klein ML. Comparison of simple potential functions for simulating liquid water. J Chem Phys 1983;79:926–935.
36. Darden T, York D, Pedersen L. Particle mesh Ewald: An N log (N) method for Ewald sums in large systems. J Chem Phys 1993;98: 10089–10092.
37. Essmann U, Perera L, Berkowitz ML, Darden T, Lee H, Pedersen LG. A smooth particle mesh Ewald method. J Chem Phys 1995;103: 8577–8593.
38. Ryckaert J-P, Ciccotti G, Berendsen HJ. Numerical integration of the cartesian equations of motion of a system with constraints: Molecular dynamics of *n*-alkanes. J Comput Phys 1977;23:327–341.
39. Berendsen HJ, Postma JPM, van Gunsteren WF, DiNola A, Haak J. Molecular dynamics with coupling to an external bath. J Chem Phys 1984;81:3684–3690.
40. Kollman PA, Massova I, Reyes C, Kuhn B, Huo S, Chong L, Lee M, Lee T, Duan Y, Wang W. Calculating structures and free energies of complex molecules: combining molecular mechanics and continuum models. Acc Chem Res 2000;33:889–897.
41. Massova I, Kollman PA. Combined molecular mechanical and continuum solvent approach (MM-PBSA/GBSA) to predict ligand binding. Perspect Drug Discov Des 2000;18:113–135.
42. Sitkoff D, Sharp KA, Honig B. Accurate calculation of hydration free energies using macroscopic solvent models. J Phys Chem 1994; 98:1978–1988.
43. Lee C, Yang W, Parr RG. Development of the Colle-Salvetti correlation-energy formula into a functional of the electron density. Phys Rev 1988;B 37:785–789.
44. Becke AD. A new mixing of Hartree-Fock and local density-functional theories. J Chem Phys 1993;98:1372–1377.
45. Binkley JS, Pople JA, Hehre WJ. Self-consistent molecular orbital methods. 21. Small split-valence basis sets for first-row elements. J Am Chem Soc 1980;102:939–947.
46. Gordon MS, Binkley JS, Pople JA, Pietro WJ, Hehre WJ. Self-consistent molecular-orbital methods. 22. Small split-valence basis sets for second-row elements. J Am Chem Soc 1982;104:2797–2803.
47. Pietro WJ, Francl MM, Hehre WJ, Defrees DJ, Pople JA, Binkley JS. Self-consistent molecular orbital methods. 24. Supplemented small split-valence basis sets for second-row elements. J Am Chem Soc 1982;104:5039–5048.
48. Naik PK, Santoshi S, Rai A, Joshi HC. Molecular modelling and competition binding study of Br- Noscapine and colchicine provide insight into noscapinoid-tubulin binding site. J Mol Graph Model 2011;29:947–955.
49. Halgren TA, Murphy RB, Friesner RA, Beard HS, Frye LL, Pollard WT, Banks JL. Glide: a new approach for rapid, accurate docking and scoring. 2. Enrichment factors in database screening. J Med Chem 2004;47:1750–1759.
50. Friesner RA, Banks JL, Murphy RB, Halgren TA, Klicic JJ, Mainz DT, Repasky MP, Knoll EH, Shelley M, Perry JK, ShawDE, Francis P, Shenkin PS. Glide: a new approach for rapid, accurate docking and scoring. 1. method and assessment of docking accuracy. J Med Chem 2004;47:1739–1749.
51. Wang J, Wang W, Kollman PA, Case DA. Automatic atom type and bond type perception in molecular mechanical calculations. J Mol Graph Model 2006;2:247–260.
52. Jakalian A, Jack DB, Bayly CI. Fast, efficient generation of high-quality atomic charges. AM1-BCC model: I I .Parameterization and validation. J Comput Chem 2002;23:1623–1641.
53. Zoete V, Meuwly M, Karplus M. Study of the insulin dimerization: binding free energy calculations and per-residue free energy decomposition. Proteins 2005;61:79–93.
54. Zoete V, Michielin O. Comparison between computational alanine scanning and per-residue binding free energy decomposition for protein–protein association using MM-GBSA: application to the TCR–p-MHC complex. Proteins 2007;67:1026–1047.
55. Gohlke H, Kiel C, Case DA. Insights into protein–protein binding by binding free energy calculation and free energy decomposition for the Ras–Raf and Ras–RalGDS complexes. J Mol Biol 2003;330: 891–913.
56. Suri C, Hendrickson TW, Joshi HC, Naik PK. Molecular insight into γ-γ tubulin lateral interactions within the γ-tubulin ring complex (γ-TuRC). J Comput Aided Mol Des 2014;28:751–763.